ICANS IX

INTERNATIONAL COLLABORATION ON ADVANCED NEUTRON SOURCES

22-26 September, 1986

PERFECT CRYSTAL AND MAGNETIC FIELD BEAM TAILORING

H. Rauch

Atominstitut der Österreichischen Universitäten, A-1020 Wien, Austria

Perfect crystals and magnetic fields are effective and coherent tools for beam tailoring. Moderate magnetic fields can cause shifts of the perfect crystal reflection curve of the order of its width, which provides the basis for gated crystal systems and for crystal resonators. Various systems for an extremely high energy or momentum resolution have been tested. They are based on an effective decoupling of the resolution from the intensity. It is shown how travelling magnetic waves can be used for an effective beam bunching from pulsed sources.

1. INTRODUCTION

Evidently the ICANS-meetings deal mainly with more intense primary neutron sources but it should be remembered that the quality of a diffraction experiment will still depend on the economy with which the available neutrons are used throughout the whole experiment. Unfortunately, at present, thermal neutrons can only be produced by a statistical slowing down process, where they become spread into a wide phase space which causes a very low density in the elementary phase space (Maier-Leibnitz 1966). There are no methods known for neutrons that give an increase of the phase space density as exist in charged particle physics (e.g. Sorenson et al. 1983, v.d.Meer 1985).

To compete with other techniques of condensed matter research, a very effective use of the available neutrons is required. The decoupling of the resolution from the intensity is an effective tool in this direction. A high resolution of one quantity - energy or momentum - is usually balanced by a worse resolution of the other. In certain cases the resolution in diffraction techniques has been increased up to a level where the objects and time scales under investigation are accessible to direct methods.

It will be shown, in separate chapters, that the combination of perfect crystal diffraction and the Zeeman energy shift due to magnetic fields can be used for novel beam tailoring devices. Although the phase space density remains unchanged, the intensity can be shifted into phase space elements which are of interest to specific experiments. Not all details can be treated in this article and the reader is referred to the cited literature.

2. RESOLUTION-INTENSITY DECOUPLING

2.1 Spin-echo systems

The spin-echo technique was established in 1972 (Mezei 1972) and is now widely used in neutron spectroscopy (Mezei 1980). It provides a decoupling of the energy resolution from the energy width of the beam by using the Larmor precession of the neutron spin to measrue the energy transfer. This method operates most effectively at small momentum transfers and reaches energy resolutions in the 10^{-4}eV range.

2.2 Nondispersive double perfect crystal systems

These systems provide in momentum space, an analog of the spin echo system which operates in energy space. The symmetrical Bragg reflection from a perfect crystal can be given in the form of the Darwin curve (e.g. Rauch & Petrascheck 1978, Sears 1978)

$$R(y) = 1 \qquad |y| \leq 1$$

$$R(y) = 1 - \sqrt{1 - \frac{1}{y^2}} \qquad |y| > 1 \qquad (1)$$

$$y = \frac{\pi(\theta - \theta_B)\sin 2\theta_B}{\lambda^2 b_c N}$$

where θ_B, b_c and N are resprectively, the Bragg angle, the coherent scattering length and the particle density. The rocking curve of a double crystal system is given by the convolution of two such reflection curves

$$I(y) = \int R_1(y')R_2(y + y')dy' \qquad (2)$$

and exhibits a width of about 2 seconds of arc. The tails can be reduced by channel-cut crystals (Bonse & Hart 1965). These systems can be used for investigations of small angle scattering from a sample placed in between the crystals (Fig.1). The related momentum transfer regime is much smaller

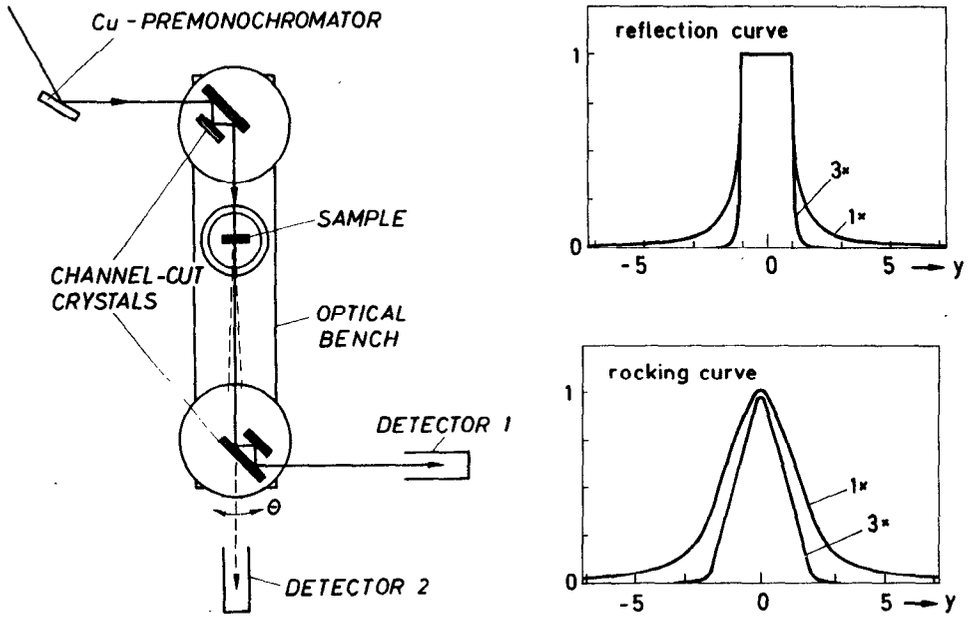

Fig.1: Experimental arrangement to demonstrate, and indication of, the action of channel-cut perfect crystals on the rocking curve of a double crystal system.

than in conventional small angle scattering instruments. The data evaluation has to take account of the slit-like geometry, as is often done in X-ray small angle scattering investigations (e.g. Glatter & Kratky 1982).

The typical momentum transfer regime ($Q = 2k\sin\theta/2 \sim k\theta$) becomes 10^{-5} Å$^{-1} \leq Q \leq 10^{-3}$Å^{-1} but the intensity remains rather high because - in principle - all neutrons reflected from the first crystal are also reflected from the second. From the accessible Q-range, follows that objects with dimensions of the order of μm can be investigated. Related experiments with neutrons using channel-cut perfect crystals can be found in the literature. Polymer blends and lamellar structures have been investigated (Schwahn et al. 1985).

An even more effective use of the available neutron intensity can be obtained by a multiple perfect crystal small angle scattering camera as shown in Fig. 2. The resolution can be varied by using symmetrical or asymmetrical cut crystals or perfect multiplate crystal systems (curved or with a temperature gradient). Intensity gains of up to a factor 100 seem to be feasible by using the full potential of this method.

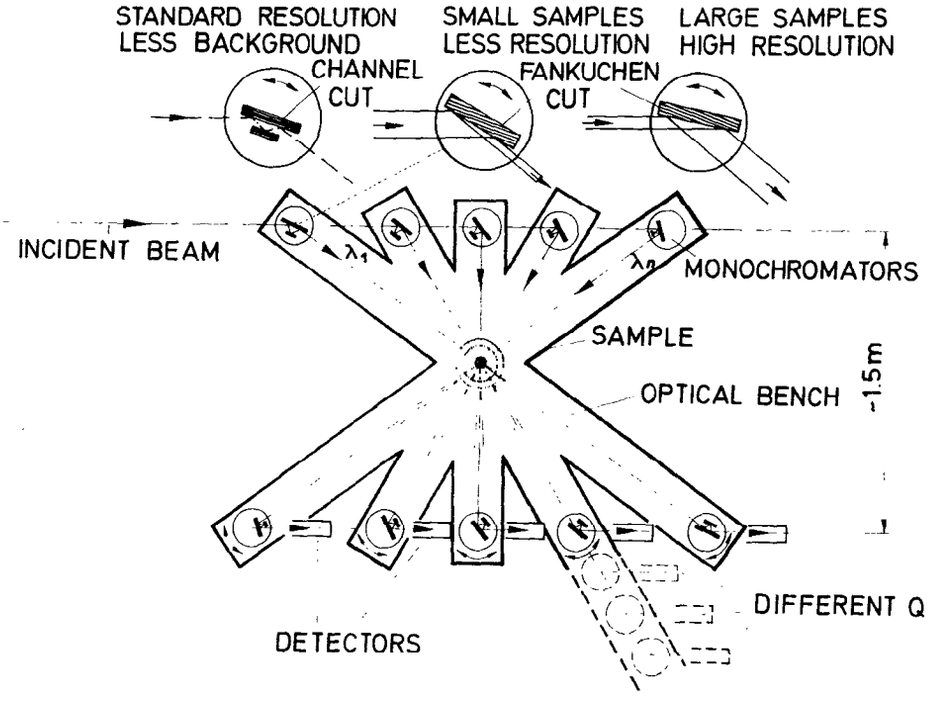

Fig.2: Proposed design of a multiple small angle scattering camera for stereoscopic investigation of samples.

2.3 Multiple Laue-Reflection (Diffraction focusing)

Even higher Q-resolutions can be achieved with a perfect crystal system when a monolithic multiplate system is used in the Laue position; that is where the lattice planes in the different plates are parallel (coherent) to each other and where the whole Pendellösung structure of the reflection curve has to be taken into account (e.g. Rauch & Petrascheck 1978, Sears 1978).

$$\frac{P_H}{P_0} = \frac{\sin^2 A\sqrt{1 + y^2}}{1 + y^2} \qquad (3)$$

$A = b_C \lambda N t/\cos\theta_B$ gives the reduced thickness of the crystal plates. This curve and the related rocking curve for a nondispersive arrangement are shown in Fig.3. The rocking curve exhibits a very narrow central peak whose width is determined by the ratio of the lattice constant divided by the thickness of the crystal ($\theta \sim d_{hkl}/t$), which is in the order of a thousandth of a second of arc (Bonse et al. 1977).

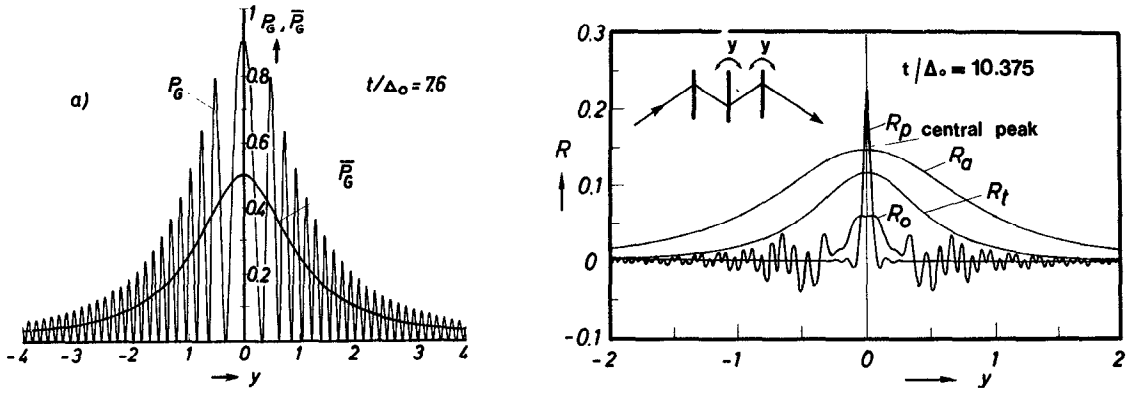

Fig. 3: Laue reflection curve and various contribution to a triple Laue rocking curve.

This effect was first observed for a monolithic two plate system (Bonse et al. 1979). In order to achieve the required high angular sensitivity for a precise rocking curve measurement a wedge was rotated around the beam axis. This produces for a wedge with an apex angle β, a beam deflection in the horizontal plane of

$$\delta = \frac{N\lambda^2 b_c}{\pi} \, tg\frac{\beta}{2} \sin\alpha. \qquad (4)$$

This trick causes a magnification factor of about 10^5 between the deflection angle δ and the rotation angle α of the wedge. The related rocking curves can also be calculated analytically, which is important for an application to small angle scattering (Petrascheck & Rauch 1984). This extremely high angular resolution can be used for small angle scattering measurements in the Q-range of $10^{-7}\text{Å}^{-1} \leq \Delta Q \leq 10^{-9}\text{Å}^{-1}$. A related measurement for the triple plate case has been reported (Rauch et al. 1983), where the diffraction of 1.8 Å neutrons at a single slit with a width of 5 mm has been observed (Fig.4).

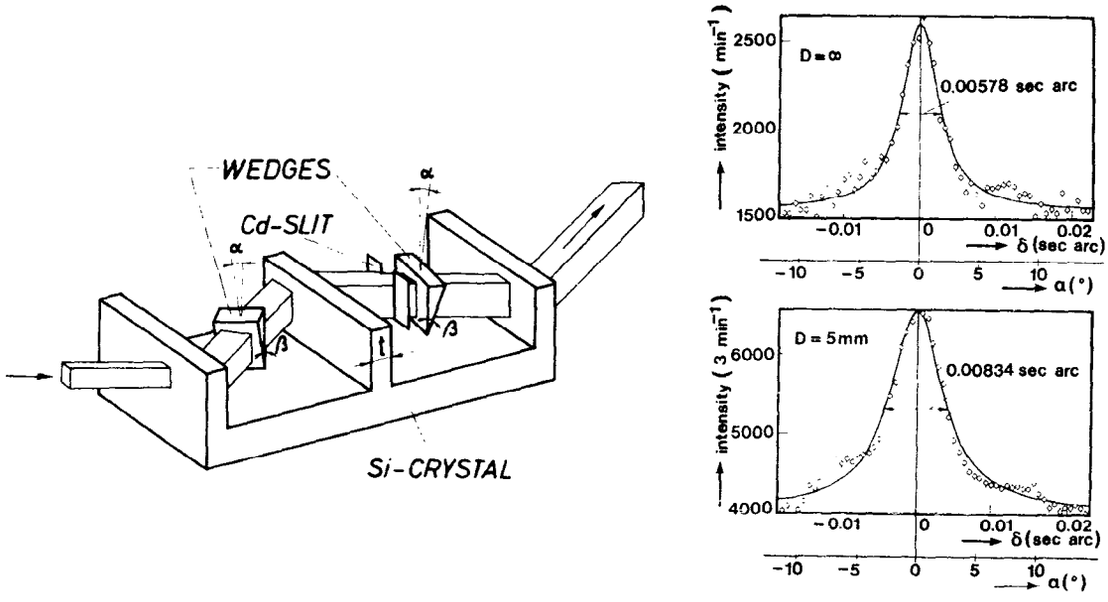

Fig.4: Sketch of the triple Laue rocking curve experiment and the measured broadening of the central peak due to single-slit diffraction from a 5 mm slit.

This behaviour can also be understood in terms of the Heisenberg uncer-

tainty relation $\Delta Q \Delta x \geq \hbar/2$. Therefore, perfect crystal extends small angle scattering investigations from the study of microscopic objects up to the observation of macroscopic systems. Applications to the investigation of macroscopic cracks or voids in bulk or for the observation of long range density fluctuations, can be envisaged.

The high angular sensitivity can also be used to give to a high energy resolution of the order of 10^{-9}eV (Zeilinger et al.1979).

2.4 Coherent magnetic resonance system

This device takes advantage of the high sensitivity achieved in neutron interferometry (Rauch et al. 1974, Bonse & Rauch 1979) and from the Zeeman energy exchange between the neutron and a Rabi-type resonance flipper (Alefeld et al. 1981). Here a real energy exchange between the neutron and the resonance flipper device takes place. This feature has been verified experimentally, using a backscattering instrument with an energy resolution ΔE better than the Zeeman energy transfer $2\mu B$. The kinetic energy changes at the entrance due to the Zeeman splitting. Inside the resonance coil, the energy quanta $\hbar\omega_1 = 2\mu B_0$ is exchanged which

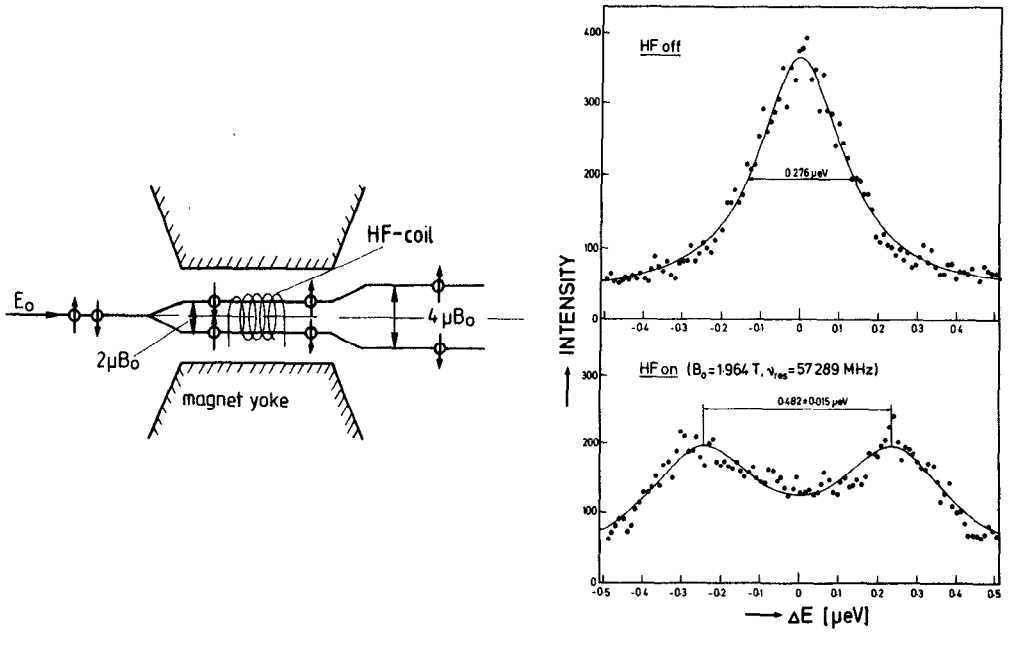

Fig. 5: Sketch of the neutron magnetic resonance system and the observed energy shift at resonance.

changes the potential (and total) energy of the neutron accordingly, and at the exit the Zeeman energy shift occurs in the same direction (Fig.5).

Inside a neutron interferometer, an energy transfer smaller than the apparent energy resolution of the system can be observed because properties of the wave function itself become measureable. In this case the total energy change and the two wave functions of both beams can be written as

$$\psi_0^{I} + \psi_0^{II} \rightarrow e^{i(\omega - \omega_{L_1})t} |-z\rangle + e^{i\chi} e^{i(\omega - \omega_{L_2})t} |-z\rangle \qquad (5)$$

This results in an intensity modulation of the beams behind the interferometer

$$I_0 \propto |\psi_0^{I} + \psi_0^{II}|^2 \propto 1 + \cos\,[\chi + (\omega_{L_1} - \omega_{L_2})t] \qquad (6)$$

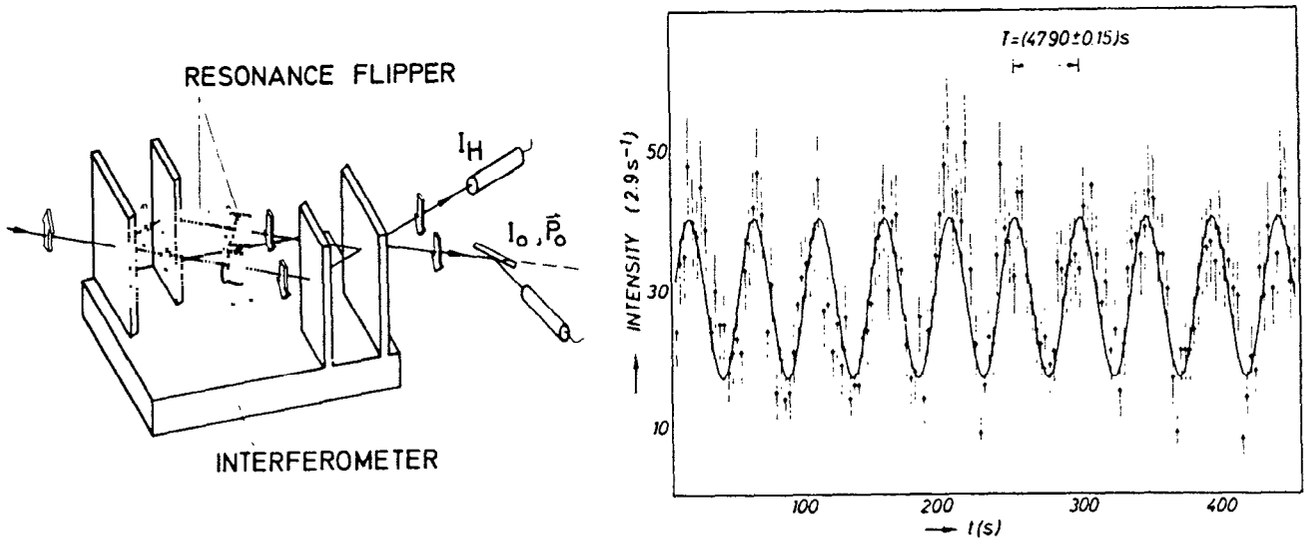

Fig.6: Experimental arrangement of the double coil quantum beat experimental which achieved an energy sensitivity of 2.7×10^{-19}eV.

where χ is a static (and hence unimportant) phase shift given by the index

of refraction. The energy transfer in both beams ($\hbar\omega_{L1}$ and $\hbar\omega_{L2}$) can be chosen to be different and then a time-dependent intensity modulation with a time constant $T = 2\pi/(\omega_{L1} - \omega_{L2})$ occurs. The result of a related experiment, where the frequency difference chosen was only 0.02 Hz and hence the beating period corresponded to an energy difference of $8.6 \cdot 10^{-17}$eV and to an energy sensitivity of $2.7 \cdot 10^{-19}$eV (Badurek et al. 1986), is shown in Fig. 6.

The extremely high momentum resolution discussed in chapter 2.3 and the extremely high energy resolution discussed in this chapter approach the limits of the uncertainty relation ($\Delta k \Delta x \geq \hbar/2$ and $\Delta E \Delta t \geq \hbar/2$).

Summarizing this general chapter: one gets three levels of energy and momentum resolution (ΔE_{exp}, ΔQ_{exp}), and in each case a strong decoupling from the energy and momentum width (ΔE_{beam}, Δk_{beam}) of the beam exists, which also means these instruments operate at a comparable intensity level.

These high resolution systems also have on the other hand distinct constraints concerning the accessible Q-range, which usually becomes more and more concentrated near Q=0.

Table 1

Resolution - Intensity Decoupling Systems

	$\frac{\Delta E_{exp}}{\Delta E_{Beam}}$	$\frac{\Delta Q_{exp}}{\Delta k_{Beam}}$
standard spectroscopy	~ 1	~ 1
	crystal and time-of flight	
high resolution spectroscopy	$\sim 10^{-4}$	$\sim 10^{-2}$
	spin-echo	*non dispersive perfect crystals*
ultra high resolution spectroscopy	$\sim 10^{-12}$	$\sim 10^{-6}$
	coherent double resonance system	*multiple Laue reflection*

3. GATED CRYSTALS

The reflection curve of perfect crystals in the Bragg position has been discussed in chapter 2.1. As can be seen from equation (1), a particular situation exists for backreflection ($\theta_B = \pi/2$) when the acceptance angle becomes rather large (the order of 1 degree). This provides the basis for back-scattering spectrometers which are used routinely for high resolution neutron spectrometry (e.g. Alefeld 1972). The Darwin curve of a perfect crystal in the reflection position can be shifted relatively either by changing the lattice constant (e.g temperature variation) or by applying a magnetic field to change the wavelength of the neutrons. This latter change can be calculated from energy conservation in the entrance field (see Fig.5)

$$H = \frac{\hbar^2 k^2}{2m} - \vec{\mu}\vec{B} \tag{7}$$

which caused the wavelength to change:

$$\lambda_{\pm} = \lambda\left(1 \mp \frac{\mu B}{2E}\right) \tag{8}$$

In the back-scattering position, where the acceptance angle becomes very large, the width of the reflection curve corresponds to a momentum transfer width of

$$\frac{\Delta k}{k} = 4N_c b_c |F| \frac{d_{hkl}}{\pi} \tag{9}$$

The shift due to a magnetic field can be written as

$$\Delta k_m = \pm \frac{\mu B m}{\hbar^2 k} \tag{10}$$

The magnetic field required to change the gate from the closed to the open position (i.e. a shift of 2 y-units) is 12.6 kG for the (111) back-reflection from silicon (λ = 6.275 Å). The proposed system and the shift of the reflection curve are shown in Fig.7. The system acts effectively only for a pulsed beam and when

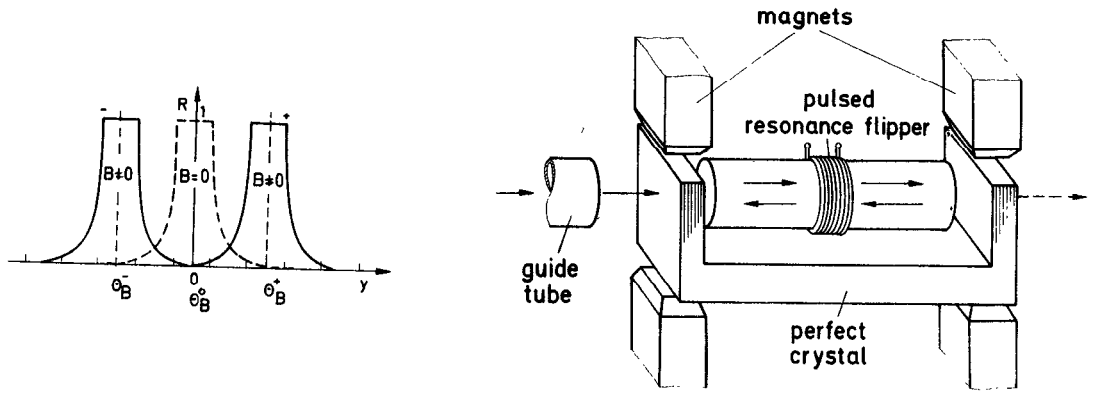

Fig. 7: Sketch of a proposed perfect crystal resonator and indication of the action of perfect crystals.

the magnetic field (or the resonance coil) is operated synchronously so as to catch neutrons between the perfect crystal plates. The version with the pulsed resonator flipper has the advantage that a stationary field at the crystal plates is sufficient. The performance of fast pulsed resonance flippers has been tested (Rauch et al. 1968, Freisleben & Rauch 1972).

The action of such a system can be increased by using a multiple backreflection crystal system as shown in Fig.8, where a temperature

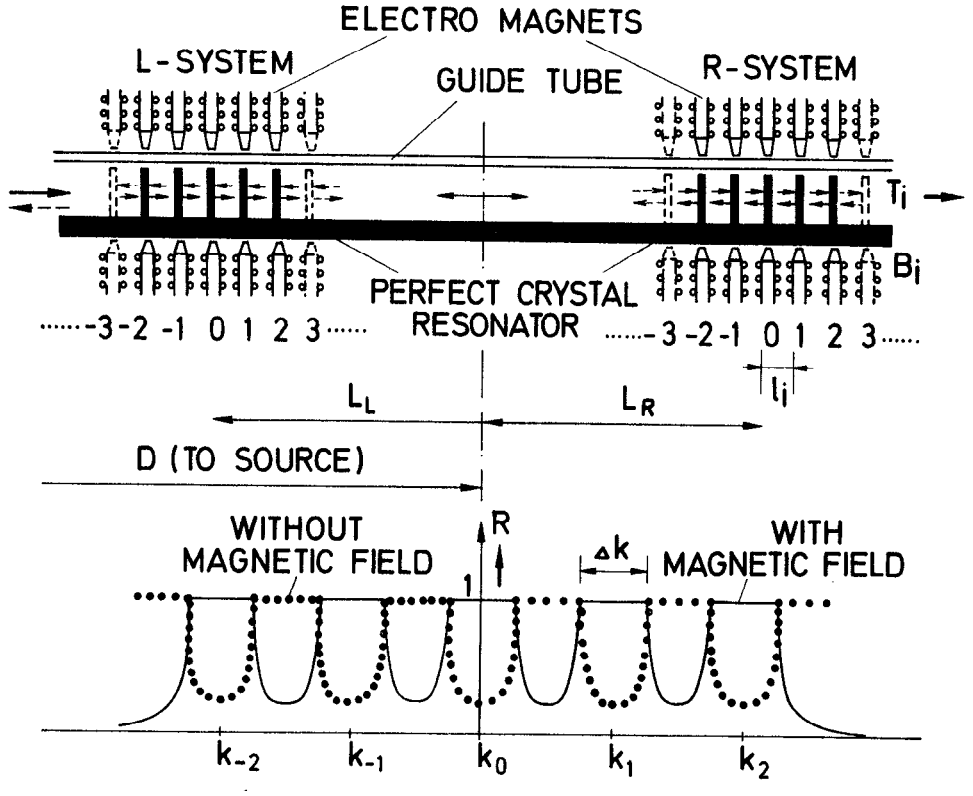

Fig. 8: The proposed multiple perfect crystal back-reflection resonator

difference is chosen to obtain a comb-shaped reflection curve which can be varied between an open and a closed position by a magnetic field (Rauch 1985). The temperature difference required for a shift of 2 in y-units (i.e. the whole width) is given as

$$\Delta T = \left[1 + \frac{\pi}{8 N_c b_c |F| d_{hkl}^2}\right]^{-1} \frac{1}{\alpha} \qquad (11)$$

where α is the linear expansion coefficient. The temperature difference for a (111) back-reflection from silicon is 8 K. Figure 8 shows a possible multiplate system, with a temperature gradient between the plates of 16°C and where the magnetic fields at the crystals can be varied in the required manner. Such devices can be used to good advantage at pulsed sources: neutrons can be caught temporarily between the crystal plates and then released under controlled conditions. Either fast switching magnets or a pulsed spin flipper between the crystal system can be used as the active element of the system. Similar systems, with a monochromatizing action, have also been discussed (Rauch 1985).

4. TRAVELLING MAGNETIC WAVE SYSTEM

The neutron magnetic resonance system, discussed in chapter 2.4 (Fig. 5), provides an energy shift of only the Zeeman energy ($2\mu B_0$). An alternative method, which so far has only been investigated theoretically, is to use a magnetic oscillator potential, with a fixed or an expanding width (w(t)), that moves along the path of a pulsed neutron beam (Fig. 9). In this arrangement, the gradient of the field acts more effectively than in the static case. Figure 9 shows a schematic layout for such a system, which could be installed along a neutron guide at a pulsed source (Rauch et al. 1985, Summhammer et al. 1986).

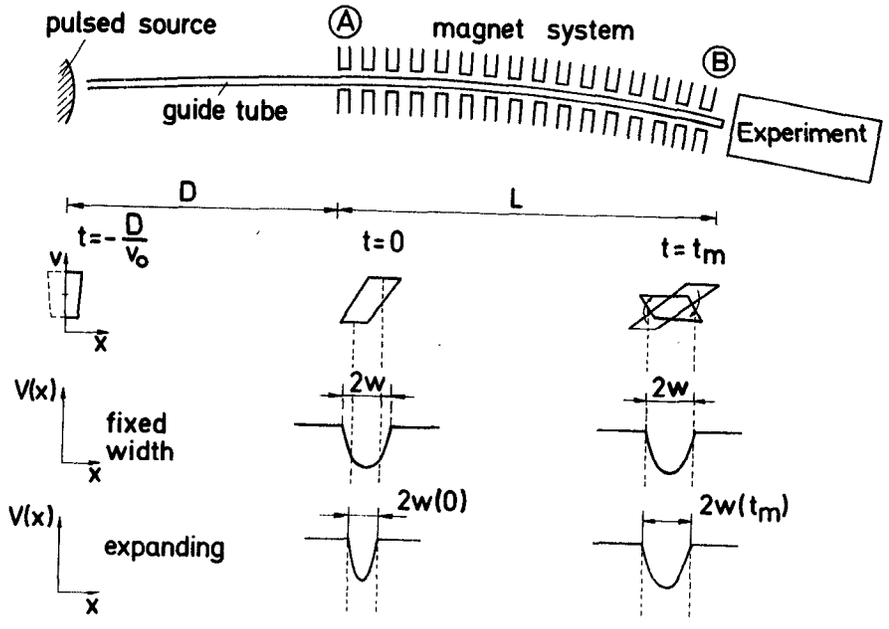

Fig. 9: Schematic layout of a travelling magnetic-wave system for beam bunching.

While passing along the beam path, the neutron feels a potential

$$V(x',t) = \pm\mu B_{max}\left(\frac{x'^2}{w^2(t)} - 1\right) \qquad |x'| \leq w(t)$$

$$= 0 \qquad |x'| \geq w(t) \qquad (12)$$

where primed variables refer to quantities in the moving frame of the potential. Neutrons in the potential and within a specific velocity band, perform an oscillatory movement. The maximum escape velocity in the reference frame is given by

$$v_{esc} = \sqrt{\frac{2\mu B_{max}}{m}} \qquad (13)$$

which reaches, for $B_{max} \tilde{}$ 10kG, a value of a few m/s and which is a factor of about 100 larger than the normal Zeeman splitting. The maximum gain factor for a fixed width potential can be written as

$$\rho = \frac{2w}{\tau V_0} \qquad (14)$$

where τ is the pulse width of the source. By means of this method a reasonable intensity gain within the specific velocity band can be achieved, as is shown in the figure 10.

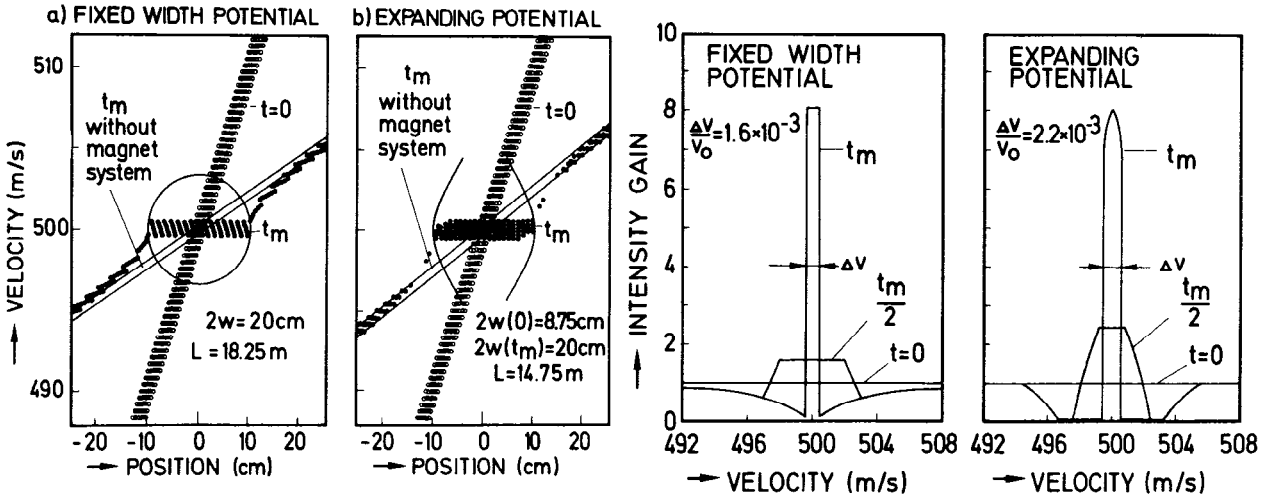

Fig. 10: Phase-space rotations of a pulsed beam for a fixed width potential and an expanding potential (left), and the related intensity gains (right) for feasible parameters (see text).

The results have been calculated for a source with a pulse width of 50μs located 5m in front of the travelling wave system, a maximum field strength of 10kG and a mean neutron velocity v_0 of 500m/s ($\lambda \sim 7.91$ Å) (which equals the velocity of the travelling wave). The action of the travelling magnetic potential corresponds to a rotation of the pulse in the x,v-phase space, hence the phase space density remains constant. Such systems will be expensive but they permit a very general tailoring of the beam pulse. Further details may be found in the references given.

The contributions of my colleagues in our institute, who are cited in the references, are gratefully acknowledged. Most of the investigations discussed in this paper were supported financially by Fonds zur Förderung der wissenschaftlichen Forschung (project S4202).

References:

Alefeld G., Kerntechnik 14(1972)15

Alefeld B., Badurek G., Rauch H., Z.Physik B41(1981)231.

Badurek G., Rauch H., Tuppinger D., Phys.Rev.A34(1986)2600.

Bonse U., Hart M., Appl.Phys.Lett.7(1965)238.

Bonse U., Graeff W., Teworte R., Rauch H., phys.stat.sol.(a)43(1977)487.

Bonse U., Graeff W., Rauch H., Phys.Lett.69A(1979)420.

Bonse U., Rauch H., (Eds.) "Neutron Interferometery" Clarendon Press Oxford, 1979.

Freisleben H., Rauch H., Nucl.Instr.Meth. 98(1972)61.

Glatter O., Kratky O., "Small Angle X-Ray Scattering", Academic Press, N.Y.1982.

Maier-Leibnitz H., Nukleonik 8(1966)5.

Meer van der, S. Rev.Mod.Phys.57(1985)689.

Mezei F., Z.Physik 255(1972)146.

Mezei F., (Ed.), "Neutron Spin Echo", Lect.Notes Physics 128, Springer Verlag, 1980.

Petrascheck D., Rauch H., Acta Cryst. A40(1984)445.

Rauch H., Harms J., Moldaschl H., Nucl.Instr.Meth.58(1968)261.

Rauch H., Treimer W., Bonse U., Phys.Lett.A47(1974)369.

Rauch H., Petrascheck, in "Neutron Diffraction (Ed.H.Dachs), Top. Current Physics 6,303, Springer Verlag 1978.

Rauch H., Kischko U., Petrascheck D., Bonse U., Z.Phys.B51(1983)11.

Rauch H., in "Neutron Scattering in the 90-ties", p.35, IAEA-Vienna 1985.

Rauch H., Summhammer J., Weinfurter H., in "Neutron Scattering in the 90-ties", p.53, IAEA-Vienna, 1985.

Schwahn D., Miksovsky A., Rauch H., Seidl E., Zugarek G., Nucl.Instr. Meth.A239(1975)229.

Sears V.F., Can.J.Physics, 56(1978)1261.

Sorenson A.H., Bonderup E., Nucl.Instr.Meth.215(1983)27.

Summhammer J., Niel L., Rauch H., Z.Physik B62(1986)269.

Zeilinger A., Shull C.G., Phys.Rev.B19(1979)3957.